

# Characterization of the tumor immune microenvironment in early-stage clear cell renal cell carcinoma (ccRCC): prognostic value of M0-macrophage enriched subtype and immune content score

Mark Farha<sup>1</sup>, Randy Vince<sup>2</sup>, Srinivas Nallandhigal<sup>2</sup>, Brittney Cotta<sup>2</sup>, Judith Stangl-Kremser<sup>2,4</sup>, Daniel Triner<sup>2</sup>, Todd Morgan<sup>2,3</sup>, Ganesh Palapattu<sup>2,3,4</sup>, Marcin Cieslik<sup>3,5,6</sup>, Ulka Vaishampayan<sup>1,3,7</sup>, Aaron Udager<sup>3,5,6</sup>, Simpa Salami<sup>2,3,6</sup>

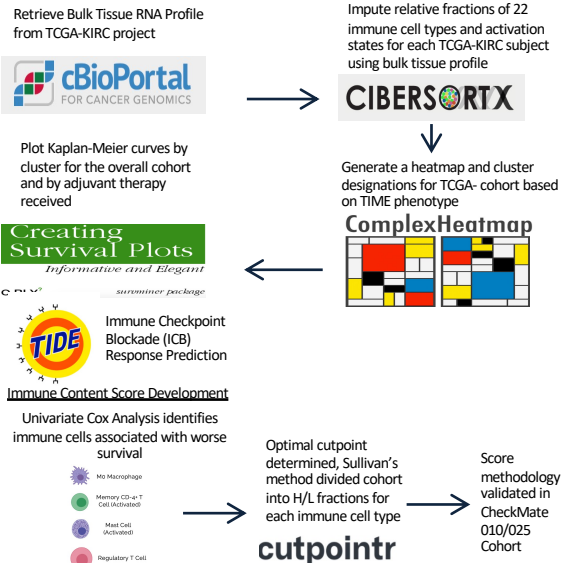
<sup>1</sup>University of Michigan Medical School, Ann Arbor, Michigan, USA.  
<sup>2</sup>Department of Urology, Michigan Medicine, Ann Arbor, Michigan, USA.  
<sup>3</sup>University of Michigan Rogel Cancer Center, Ann Arbor, Michigan, USA.  
<sup>4</sup>Department of Urology, Medical University of Vienna, Vienna, Austria.  
<sup>5</sup>Department of Pathology, Michigan Medicine, Ann Arbor, Michigan, USA.  
<sup>6</sup>Michigan Center for Translational Pathology, Michigan Medicine, Ann Arbor, Michigan, USA.  
<sup>7</sup>Department of Medicine, Michigan Medicine, Ann Arbor, Michigan, USA



## Purpose/Objective

Cancer of the kidney and renal pelvis is one of the most commonly diagnosed malignancies in the world, with ccRCC accounting for the majority of cases. Recurrence after nephrectomy is a common phenomenon, with likelihood of recurrence increasing with increasing tumor size. The adjuvant treatment paradigm is rapidly evolving, with first generation immunotherapies giving way to targeted therapies and most recently immune checkpoint blockade (ICB). Appropriate selection criteria for those who may benefit most from adjuvant ICB therapy is limited to traditional clinical and pathologic characteristics. In this study, we elucidate the immune composition of a ccRCC cohort within the TCGA project presenting with localized disease, and develop an immune content score to predict ICB response, which we then validate in a Nivolumab treated arm of the CheckMate 010/025 trials

## Methods



## Results

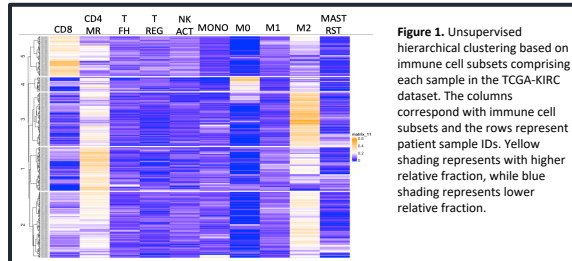


**Figure 1.** Unsupervised hierarchical clustering based on immune cell subsets comprising each sample in the TCGA-KIRC dataset. The columns correspond with immune cell subsets and the rows represent patient sample IDs. Yellow shading represents with higher relative fraction, while blue shading represents lower relative fraction.

**Table 1.** Demographic, pathologic, and molecular characteristics of non-metastatic patients in the TCGA-KIRC cohort, organized by TIME cluster.

	Cluster 1 (N = 77)	Cluster 2 (N = 116)	Cluster 3 (N = 94)	Cluster 4 (N = 25)	Cluster 5 (N = 70)
Median Age (years)	60.9	61.8	59.4	62.4	60.2
Gender (M/F, %)	62/38	59/41	72/28	72/28	61/39
Race (W/B/A/NA, %)	96/4/0/0	95/3/1/2	93/3/2/2	96/0/4/0	96/1/3/0
Laterality (R/L, %)	61/39	53/47	53/47	60/40	46/54
Mutation Count (Min, Median, Max)	1, 48, 553	1, 48, 708	1, 48, 409	1, 48, 89	1, 48, 93
Fraction Genome Altered (Mean %)	15.9	13.3	16.1	23.4	15.9
Lab Parameters (I/L/WNL/NA %)					
Serum Ca	3/44/23/30	1/41/27/32	0/49/17/34	0/60/16/24	1/43/26/30
Hemoglobin (Hgb)	1/52/32/14	2/46/39/14	1/45/33/21	0/56/36/8	0/56/39/6
Platelets (PLT)	5/10/68/17	8/12/66/15	3/6/69/21	0/20/68/12	6/9/77/9
White Blood Cells (WBC)	34/0/48/0	38/3/44/16	40/1/36/22	32/4/52/12	37/1/54/8
Lymph Nodes ±(%)*	0	8	16	10	23
Grade (%)					
G1	5	3	0	4	1
G2	57	46	54	32	37
G3	25	41	39	52	46
G4	13	9	5	12	16
Pathologic Stage (%)					
I	60	53	68	40	49
II	12	11	11	12	16
III	27	35	19	48	34
IV	1	0	1	0	1
Pathologic T Stage (%)					
T1, T1a, T1b	6, 26, 27	4, 32, 18	7, 38, 22	0, 20, 24	0, 20, 29
T2, T2a, T2b	10, 1, 0	7, 3, 1	11, 0, 0	12, 0, 0	14, 1, 1
T3, T3a, T3b, T3c	0, 17, 10, 0	1, 24, 8, 2	1, 17, 2, 0	0, 16, 28, 0	0, 21, 11, 0
T4	1	0	1	0	1
Mutations (% WT, MUT, NA)					
TP53	90/1/9	90/4/6	87/2/11	88/0/12	90/0/10
VHL	44/48/9	41/53/6	35/54/11	52/36/12	44/45/10
PBRM1	56/35/9	62/32/6	59/31/11	52/36/12	74/16/10
SETD2	75/16/9	87/7/6	82/7/11	76/12/12	84/6/10
TCEB1	91/0/9	93/1/6	88/1/11	88/0/12	89/1/10
Predicted ICB Response (%)	27	23	20	4	34

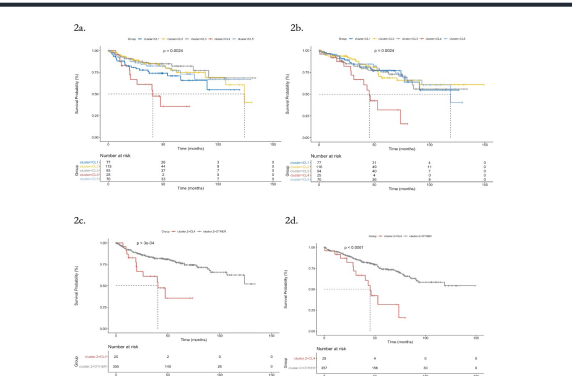


**Figure 2a-d.** Survival analyses. Kaplan-Meier curves for progression free survival (PFS) (2a) and overall survival (OS) (2b) for each cluster in the TCGA-KIRC cohort are shown. Pairwise log-rank comparisons were conducted for each curve. Kaplan-Meier curves for PFS) (2c) and OS) (2d) for grouped clusters 1, 2, 3, and 5 combined and labeled as OTHER compared with cluster 4 are shown. Pairwise log-rank comparisons are included for each curve.

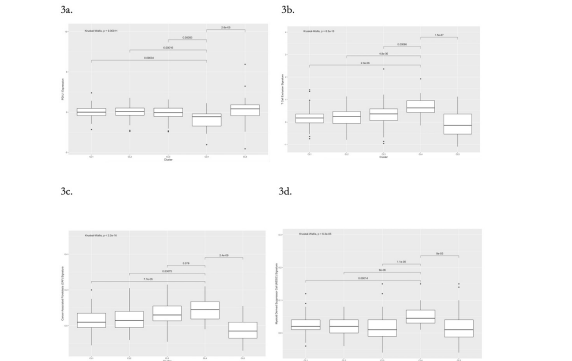


**Figure 3a-d.** Box plots representing key tumor immune microenvironment parameters by cluster in the non-metastatic TCGA-KIRC cohort. Data presented in this figure is from the tumor immune dysfunction and exclusion (TIDE) module. PD-L1 expression Z-scores (3a), and signatures for T-Cell Exclusion (3b), and prevalence of cancer associated fibroblasts (CAFs) (3c), and myeloid derived suppressor cells (MDSs) (3d) are included. Global Kruskal-Wallis p-value, as well as individual pairwise Wilcoxon test p-values for pairwise tests between cluster 4 and the other individual clusters are displayed.

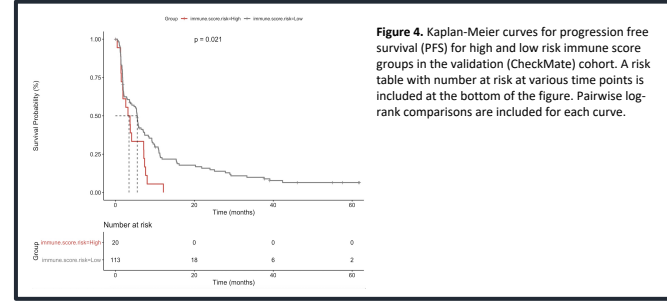


**Figure 4.** Kaplan-Meier curves for progression free survival (PFS) for high and low risk immune score groups in the validation (CheckMate) cohort. A risk table with number at risk at various time points is included at the bottom of the figure. Pairwise log-rank comparisons are included for each curve.

One cluster was characterized by macrophage enrichment, with a distinct cluster highly infiltrated with M0 macrophages (Figure 1). This cluster had a larger fraction of the genome altered, higher grade and stage, and a lower predicted response rate to ICB (Table 1). Kaplan-Meier estimates demonstrated that members of the M0-Hi demonstrated worse PFS and OS in comparison to other clusters (Figure 2). This cluster also had decreased PD-L1 expression, and a higher T-cell exclusion, cancer associated fibroblast (CAF) and myeloid derived suppressor cell (MDS) signature (Figure 3). An immune score was developed using the immune infiltration of this cluster. Nivolumab treated patients in a separate cohort (CheckMate 010/025) classified as high-risk by this immune score demonstrate shorter PFS (Figure 4).

## Conclusion

In this study we demonstrated the prognostic and predictive significance of the TIME in ccRCC. We developed and validated an immune cell signature based on transcriptomic data to risk stratify patients with ccRCC and predict response to immunotherapy. Pending further prospective validation, this signature has the potential to improve prognostication of patients with ccRCC and identify those patients most suitable for immunotherapy in the adjuvant and/or advanced disease setting.

## References/Acknowledgements

References available on request. This research was funded by the National Institutes of Health T35 grant number HL00796035 (MF). A.M.U., G.S.P., S.S.S., T.M.M. are supported by the University of Michigan Health System-Peking University Health Science Center (UMHS-PUHSC) Joint Institute (JI). S.S.S. is supported by the Robert Wood Johnson Foundation as part of the Harold Amos Medical Faculty Development Program (AMFDP). S.S.S. is supported in part by the Urology Care Foundation Rising Stars in Urology Research Award Program and Astellas, Inc. S.S.S. is supported by P30CA046592. A.M.U. is supported by the Department of Defense (W81XWH-19-1-0407) and National Institutes of Health (P50 CA186786, U01 CA232931, and R37 CA222829).

